TM70-2015-2

TECHNICAL MEMORANDUM

Bellcomm

BELLCOMM, INC.
955 L'ENFANT PLAZA NORTH, S.W. WASHINGTON, D.C. 20024

COVER SHEET FOR TECHNICAL MEMORANDUM

TITLE- A Secondary Ejecta Explanation of a Lunar Seismogram

TM- 70-2015-2

DATE- March 17, 1970

FILING CASE NO(S)- 340

AUTHOR(S)- G. K. Chang
P. Gunther
D. B. James

FILING SUBJECT(S)- Lunar Seismogram
(ASSIGNED BY AUTHOR(S)- Apollo 12
Secondary Ejecta

ABSTRACT

It has been suggested that the seismograph recording of the Apollo 12 LM impact was the result of a spray of secondary ejecta around the seismometer rather than the result of seismic waves propagated through the moon. We have made a theoretical study of the ballistic trajectories, plausible angular distributions and seismic signals to be expected from such a spray. Secondary ejecta cannot account for signals arriving earlier than 45 seconds, but could explain the remaining portion of the signal provided that the angular distribution of the secondary ejecta are assumed to peak sharply in the vertical direction. Hence, it is concluded that one can neither prove nor disprove the hypothesis that a substantial portion of the signal is due to secondary ejecta.

The planned S-IVB impact at a greater distance may resolve some of the ambiguity. If the signal contains a contribution due to the secondary ejecta then there should be a discernible difference between the onset signal, corresponding to a seismic propagation velocity of 3-4 km/sec measured by Latham, and a later signal whose arrival corresponds to a flight velocity of 1.68 km/sec. Additionally, the secondary ejecta hypothesis indicates that the time of occurrence of the broad peak should scale as the square root of the distance if the angular distribution is assumed to be the same as for the LM impact.

Since meteoroid impact should give an angular distribution similar to that from an S-IVB impact, the debris from their secondary ejecta could give equivalent signals. The ejecta model proposed here may be more applicable to meteoroids than to the LM, since the secondary ejecta due to meteoroid impact are expected to peak at higher angles.

SEE REVERSE SIDE FOR DISTRIBUTION LIST

DISTRIBUTION

COMPLETE MEMORANDUM TO

CORRESPONDENCE FILES:

OFFICIAL FILE COPY
plus one white copy for each additional case referenced

TECHNICAL LIBRARY (4)

NASA Headquarters
R. J. Allenby/MAL
D. A. Beattie/MAL
E. Christensen/MAL
M. Dubin/SG
R. J. Green/MAL
T. A. Keegan/MA-2
B. Milwitzsky/MAL
W. T. O'Bryant/MAL
R. A. Petrone/MA
L. R. Scherer/MAL
H. J. Smith/SS
W. E. Stoney/MA

Ames Research Center
D. E. Gault/SSP
C. P. Sonett/SS

Goddard Space Flight Center
J. A. O'Keefe

Jet Propulsion Laboratory
L. D. Jaffe/320

Manned Spacecraft Center
P. B. Burbank/TG
A. J. Calio/TA
J. W. Dietrich/TH3
P. Gast
R. Johnston/PA
H. H. Schmitt/CB

California Institute of Technology
D. Anderson
E. M. Shoemaker

Columbia University
M. Ewing
G. V. Latham

COMPLETE MEMORANDUM TO

Cornell University
T. Gold

Johns Hopkins University
A. H. Marcus

Massachusetts Institute of Technology
F. Press
E. Simmons

Stanford University
R. Kovach

University of California/Los Angeles
W. M. Kaula

University of California/San Diego
H. Urey

University of California/Santa Barbara
G. J. F. MacDonald

University of Hawaii
G. Sutton

Bellcomm, Inc.
G. R. Andersen
D. R. Anselmo
A. P. Boysen, Jr.
J. O. Cappellari, Jr.
C. L. Davis
F. El-Baz
D. R. Hagner
W. G. Heffron
H. A. Helm
J. J. Hibbert
N. W. Hinners
T. B. Hoekstra
B. T. Howard
D. B. James
J. A. Llewellyn
H. S. London
E. D. Marion
J. L. Marshall
K. E. Martersteck
R. K. McFarland
J. Z. Menard
B. G. Niedfeldt

DISTRIBUTION LIST (CONT'D.)

Complete Memorandum to

Bellcomm, Inc.
J. J. O'Connor
G. T. Orrok
J. T. Raleigh
P. E. Reynolds
I. M. Ross
J. A. Saxton
F. N. Schmidt
R. L. Selden
P. F. Sennewald
R. V. Sperry
A. W. Starkey
W. B. Thompson
J. W. Timko
R. L. Wagner
M. P. Wilson
All Members Departments 1033 and 2015
Department 1024 File

BELLCOMM, INC.
955 L'ENFANT PLAZA NORTH, S.W. WASHINGTON, D. C. 20024

SUBJECT: A Secondary Ejecta Explanation of a Lunar Seismogram - Case 340

DATE: March 17, 1970

FROM: G. K. Chang
P. Gunther
D. B. James

TM-70-2015-2

TECHNICAL MEMORANDUM

Introduction

Immediately after the rendezvous of the Apollo 12 LM with the CSM the separated LM was commanded to perform a burn which caused it to impact the lunar surface about 75.9 km uprange of a previously deployed ALSEP Passive Seismic Experiment (PSE). A few seconds after the impact of the LM the seismometer began to record a broad band wave train centered at about 1 Hz. The present estimate of the first signal arrival (23 sec.) is still being refined by a detailed examination of the magnetic tapes. The amplitude built up to a broad maximum at six-seven minutes and then slowly died away over the next 50 minutes (see Figure 1). Since that time a number of similar events, believed to be due to meteoroid impacts in the vicinity of the landing site, have also been recorded.

Current seismic theories attempting to explain these signals require the assumption of lunar Q's in excess of 2500, much higher than anything observed on earth. In addition, a number of people have suggested that the unusual signals may have been caused by the rain of secondary ejecta, thrown up by the impacting LM, around the PSE. These secondary ejecta may have resulted from a single impact crater or from multiple impact craters created by the low angle impact of the LM (less than 4° from the horizontal). It is plausible that the recorded seismometer signal due to LM impact may be due to both seismic and secondary ejecta sources.

In this paper we investigate the ejecta hypothesis in detail assuming that only a single impact crater has resulted. We calculate the allowed trajectories and travel times, investigate plausible angular distributions and particle densities, and attempt to model the seismic signals which would be observed when lunar dust particles rain down on the lunar surface close to the PSE.

Since the last two, the particle density distributions and the modeling of the seismic signals, require assumptions which are difficult if not impossible to verify due to lack of experimental data; we are unable either to prove or disprove the hypothesis. However, we are able to point out some characteristics which such signals must have and which may be used to test the hypothesis after the examination of future signals with other LM and S-IVB impacts.

Allowable Trajectories

In Figure 2 we show the geometry of possible trajectories connecting the LM and the seismometer, for both the curved moon and the flat moon approximation. We have found that the flat moon approximation is mathematically simpler and adequate, and we will discuss it here. The required expressions for the curved moon case are derived in the appendix, and only the results will be discussed here.

Following the nomenclature of Figure 2, the velocity and time of flight of a particle traveling between the point of LM impact A and the seismometer B can be derived from mechanics as follows:

$$\frac{V \sin \theta}{g} = t/2 \qquad (1)$$

$$(V \cos \theta)t = X \qquad (2)$$

where

V = magnitude of the particle velocity at points A and B

g = acceleration due to lunar gravity

θ = elevation angle of the trajectory

X = distance between A and B.

Solving for V and t gives

$$V = \sqrt{\frac{Xg}{\sin 2\theta}} \qquad (3)$$

$$t = \sqrt{\frac{2X}{g} \tan \theta} \qquad (4)$$

Similar but more complex expressions are derived for a curved moon in the Appendix. The equivalent of expression (3) is worth examining. From the Appendix

$$W = \frac{-\tan \theta}{\tan(\theta+f)} \qquad (5)$$

$2f = 2.5°$ is the central angle between A and B, while W is a non-dimensional energy parameter which is defined as

$$W \equiv \frac{V^2 R_0}{\mu} - 1 = 1 - \frac{R_0}{a}$$

where R_0 is the lunar radius, a is the semi-major axis of the ellipse and μ is the lunar gravitational constant. Observe that

$W = -1$ for V = zero

$W = 0$ for V = circular velocity

$W = +1$ for V = parabolic escape velocity

$W > 1$ for hyperbolic escape velocities

Figure 3 and expression (5) illustrate the allowable trajectories. The earliest particle to arrive travels along a circular trajectory at the surface of the moon with the orbital velocity of 1.68 km/sec. Thus the earliest arrival time is given by $2fR_0/1.68 = 45$ seconds. There is no way that a ballistic particle can get to the PSE faster than this on a solid moon. Equation (5) allows for faster trajectories, but these travel through the moon.

As the ejection angle θ rises from zero, the required velocity to reach B drops off until an angle of $45°-f/2$ is reached where the velocity is a minimum. This is equivalent to the well-known solution for minimum energy trajectory, $\theta=45°$, for a flat moon. In this particular case the velocity has fallen off from 1.68 km/sec (5510 fps) to .35 km/sec (1140 fps). The

trajectory follows an ellipse whose occupied focus is at the center of the moon and the vacant focus is mid-point between A and B. The flight time is approximately five minutes. Further increase in the ejection angle causes a symmetric increase in velocity until at $2(45°-f/2) = 90°-f$ we again reach 1.68 km/sec (circular velocity). The trajectory now follows a symmetric ellipse where the line AB is coincident with the minor axis of the ellipse and the flight time has risen to 89 minutes. Subsequent increase in the ejection angle gives rise to further increase in velocity and time of flight with long arc trajectories (i.e., more of the ellipse is above the moon than below), until we reach escape velocity and a parabolic trajectory at an ejection angle of $90°-f/2$.

Further increase in the ejection angle gives trajectory solutions which are hyperbolic with velocities greater than escape but which require the particle to go through infinity before reaching the PSE. These trajectories occupy ejection angles from $\theta=90°-f/2$ to $\theta=180°-f/2$ where again we have a parabolic trajectory.

The small angle between $180°-f/2$ and 180° allows a series of high velocity trajectories, $V_{circular} < V < V_{escape}$, which give retrograde paths from A to B and are long arc trajectories. Since the shortest of these, $\theta=180°$, takes 108 minutes to cover the journey, they are of little interest in this problem. Indeed, we are really only interested in those trajectories between $\theta=0°$ and $\theta=90°-f$ since the seismic record disappears into the noise after about one hour. Thus, if we are to get particles falling around the seismometer, we require only the LM to accelerate particles to velocities between .35 and 1.68 km/sec into the forward quadrant. The seismometer is only a few degrees off the flight path of the incoming LM; any peaking of particles in azimuth would affect the analysis below in a direction favorable to the secondary ejecta hypothesis.

Particle Density Distributions

Particle density is defined as the number of particles per second impacting unit area about the seismometer. Figure 4 shows the unweighted density, n(t), i.e., assuming isotropic ejection of particles and uniform distribution of velocities between the minimum energy velocity of .35 km/sec and the circular orbit velocity of 1.68 km/sec. The equation for particle density, using the flat moon approximation, is (see Appendix)

$$n(t) = n_{ME} \cdot 2 \cos^2 \theta$$

$$= n_{ME} \cdot \frac{2}{1+(t/t_{ME})^4} \qquad (6)$$

where $t_{ME} = \sqrt{2X/g}$ is the time of flight of the minimum energy trajectory and n_{ME} is the corresponding absolute particle density, whose value is discussed later. The curved moon solution differs primarily for small t, with n(t) having a maximum at t=2.5 minutes. For t>8 minutes, n(t) decreases approximately as t^{-4}. Equation (6) reflects the fact that t increases more rapidly for large θ than for small θ; also for an isotropic distribution, the number of particles ejected decreases as cos θ.

Instead of number of impacting particles, one can consider the impacting energy. The unweighted energy density, e(t), is

$$e(t) = \frac{m}{2} V^2 n(t)$$

where m is the mass of individual particles, discussed later. For a flat moon this reduces, using (3) and (4), to

$$e(t) = e_{ME} \cdot \cot \theta$$

$$= e_{ME} \cdot (t_{ME}/t)^2 \qquad (7)$$

where $e_{ME} = \frac{1}{2} m V_{ME}^2 n_{ME}$ is the energy density for the minimum energy trajectory. The curved moon solution (Figure 4) is very close to the flat moon except at small t where a steep rise occurs.

The unweighted particle and energy densities do not fit the actual seismogram. The fit can be improved by employing an appropriate anisotropic distribution. If the elevation angle distribution is $p(\theta)$, then the weighted particle density, $N(t)$, is simply

$$N(t) = p(\theta) \cdot n(t) \tag{8}$$

Similarly the weighted energy density is

$$E(t) = p(\theta) \cdot e(t) \tag{9}$$

The case when $p(\theta)$ has the form $\sin^k\theta$ is discussed in the Appendix; for $k=2$ the maximum density occurs when $t=t_{ME} \simeq 5$ minutes. If we substitute the actual seismogram for the left hand sides of equations (8) and (9) and solve for $p(\theta)$, we obtain the angular distribution which will exactly fit the seismogram (except for times less than 45 seconds), as shown in Figure 5. The extended tail of the seismogram causes these distributions to be extremely skewed toward 90°. At very low and very high angles, abrupt changes occur. The behavior at $\theta=0$ results from the fact that the seismogram is non-zero at the minimum ballistic arrival time but the particle density is zero. Conversely, for large θ (long times) the signal becomes lost in the noise, but the particle density is non-zero.

Seismic Signals Expected

So far we have discussed the possible trajectories, travel times and the form of the number density and energy density of particles to be expected in the vicinity of the seismometer. Now we must face the question whether there are enough particles and whether they have sufficient energy to cause the observed signal.

At the Apollo Lunar Science Conference it was stated that the average size of lunar dust particles is 60μ with an average mass of 3×10^{-7} gms (assuming a density of 3 and spherical shape). If we assume further that the impacting LM accelerated its own mass, approximately 3×10^{6} gms, in dust particles up to velocities between .35 km/sec and 1.68 km/sec, which is energetically

feasible, and that all particles were the same size (60μ), then we would have 10^{13} particles. The value of the constant n_{ME} in equation (6) (see Appendix) is thus .08/m^2/sec which leads to particle densities at 4-5 minutes of about .1/m^2/sec falling in the vicinity of the seismometer. In order to explain the seismogram, in the regions of both high and low signal level, one would require peak particle numbers of the order of 100/sec and need to detect signals from impacts up to 17 meters (56 feet) away. Thus we have to determine whether a .3 μgm particle traveling at velocities between .35 km/sec and 1.68 km/sec would have sufficient energy to be observed.

McGarr, Latham and Gault[1] provide some data obtained from the Ames Research Center light gas gun facility which are relevant to our discussion here. Their Figure 4a shows the maximum acceleration at the surface of a loose sand target at 2 feet from the impact point. The least squares line through the eight shots shows that acceleration varies as $E^{1/3}$, where E is the kinetic energy of the impacting particles.

Using their data for the two geophones normalized to the same distance, together with their measured signal periods, we have calculated the displacement at 2 feet. These data are plotted in Figure 6A. A line of the form $E^{1/3}$ presents a good fit to the data. Extrapolation to the energy range of interest, between 1.7×10^2 ergs and 4.2×10^3 ergs, gives displacements between 4 and 12 nanometers at a distance of 2 feet, as shown in Figure 6B. Since the seismometer is sensitive to signals of less than one nanometer, it would appear that the signals are large enough if the attentuation in the lunar regolith between the impact point and the seismometer is not too large. In the same paper McGarr, et al, refer to their previous work where seismic signals in loose sand falls off as $\frac{e^{-\gamma r}}{r^2}$, where r is the distance from the seismometer and the attenuation constant γ is inversely proportional to Q. If the factor $e^{-\gamma r}$ is ignored we find that as the area of integration is increased, the total energy/sec in the vicinity of the seismometer increases as log r. In order to obtain a sufficient signal we had previously estimated that signal responses over a radius of 17 meters would be required. Since the wavelength of the signals measured by McGarr, et al, was approximately 0.15 meters this would require a Q of about 50. To be able to detect a seismic signal from these particles, we had to assume

that seismic displacement varies as $E^{1/3}$. However, with the $E^{1/3}$ assumption, the signal amplitude falls off as $t^{-3.3}$, much too fast to be compensated by any plausible elevation angle distribution. The assumption of E dependence, with a signal falling off as t^{-2}, gives a better fit.

The McGarr, et al, data show $E^{1/3}$ dependence; however, theory based on scaling laws[2] supports E dependence. The apparent difference arises from the fact that the relaxation time, which is supposed to scale as $E^{1/3}$, was in practice virtually independent of energy. This may be because the mechanism of an explosion differs from the slowing up of a small projectile in sand. Indeed a very crude billiard ball collision model of the slowing up process indicates that the time of slowing up would be dominated by the last and the next-to-last collisions. The time between these collisions would be proportional to the mean free path and inversely proportional to the final velocity of particles whose energy could no longer produce free motion in the particles. Both parameters are functions of the soil characteristics, not of the velocity of the incoming particle, and hence the slowing up time would be independent of the velocity and energy of the incoming particle.

Conclusions

We have shown that it is feasible to obtain particle trajectories which give rise to seismic signals of the proper duration. Any signal arriving earlier than the 45 seconds required for a particle in circular orbit to reach the PSE must be due to other causes, most probably seismic propagation. Since examination of the magnetic tapes presently points to an onset time of 23 seconds[3], the first 22 seconds of the recorded signal cannot be due to secondary ejecta.

We have also shown that if the experimental results of McGarr, et al, can be extrapolated over seven orders of magnitude, then the signals due to microgram impacts can produce detectable signals in the seismometer. Since these signals will be arriving successively from different directions, we would expect similar signals on all three axes which are phase incoherent, as actually observed by Latham. Since the time of interaction of an impacting particle with the lunar surface is very short ($\sim$ one millisecond), we would also expect the signals for the Apollo 13 LM impact event to be at the upper limit of the short period seismometer frequency response.

Some predictions can also be made about the position of the broad peak, if the seismic record is primarily due to particles. If for S-IVB impacts the angular distribution of the particles is similar to that assumed here for the LM, then the position of the peak will be delayed by a time which scales as $\sqrt{x}$, where x is the distance between the impact point and the seismometer.

Since meteoroid impacts will give angular distributions similar to those from S-IVB impacts, then the debris from their secondary ejecta could give equivalent signals. One cannot use the argument that because we see similar meteoritic impact events then the signal cannot be due to ejecta. The ejecta model fits the meteoroid case better than the LM case because we would expect the debris to be peaked at high angles leading to signals which slowly rise and then fall.

Finally, since we have had to make assumptions which are difficult to prove, especially relating to number of particles that are accelerated to the required velocity and also the size of signals that microgram particles will generate in a seismometer, we must conclude that the hypothesis that part or all of the signals are caused by ejecta is neither proved nor disproved. Clearly if the S-IVB impact produces a seismogram and its impact point is 200 km distant, as planned, the onset time predicted by a propagation mechanism will be 60 seconds earlier than that predicted by an ejecta hypothesis. This time difference should permit identification of the dominant mechanism.

G. K. Chang
G. K. Chang

P. Gunther
P. Gunther

D. B. James
D. B. James

2015-GKC
1033-PG -jf
2015-DBJ

Attachments
References
Appendix
Figures 1 - 6

REFERENCES

1. McGarr, A., Latham, G. V., and Gault, D. E., "Meteoroid Impacts as Sources of Seismicity on the Moon," JGR 74, 5981 (1969).

2. Cole, R. H., "Underwater Explosions," Princeton University Press, Princeton, New Jersey, 1948.

3. Latham, G. V., et al, "Passive Seismic Experiment," Science, 167, 455, (1970).

APPENDIX

MATHEMATICAL ANALYSIS

1. Trajectory Analysis

The following analysis ignores the angular rotation of the moon, the effect of which is not significant. Consider first the case where the trajectory between A and B (see Figure 2) represents the short arc of the ellipse. Let f be the central angle between LM and apolune, so that π-f is the true anomaly. Given f, θ, and R_0, one can determine the trajectory parameters, a, e, and the ejection velocity V as follows. From the energy equation,

$$V^2 = \mu\left(\frac{2}{R_0} - \frac{1}{a}\right) \tag{1}$$

Defining the non-dimensional parameter

$$W = \frac{V^2 R_0}{\mu} - 1 \tag{2}$$

we get

$$W = 1 - \frac{R_0}{a} \tag{3}$$

or

$$a = \frac{R_0}{1-W} \tag{4}$$

The flight path angle of an elliptic trajectory is given by

$$\tan\theta = \frac{e \sin f}{1-e \cos f} \tag{5}$$

Solving for e gives

$$e = \frac{\sin\theta}{\sin(\theta+f)} \tag{6}$$

The formula for radial distance yields

$$R_0 = \frac{a(1-e^2)}{1-e\cos f} \tag{7}$$

or, from (3),

$$W = -e\,\frac{\cos f - e}{1-e\cos f} \tag{8}$$

Substituting (6) gives

$$\frac{\cos f - e}{1 - e\cos f} = \frac{\sin(\theta+f)\cos f - \sin\theta}{\sin(\theta+f) - \sin\theta\cos f} = \frac{\cos(\theta+f)}{\cos\theta} \tag{9}$$

so that from (6) and (8)

$$W = -\frac{\tan\theta}{\tan(\theta+f)} \tag{10}$$

or, using (2),

$$V = \sqrt{\frac{\mu}{R_0}\,(1-\tan\theta\cot(\theta+f))} \tag{11}$$

The minimum energy ellipse, denoted hereafter by the subscript ME, can be obtained by minimizing (10). Differentiating and equating to zero leads to

$$\theta_{ME} = \frac{\pi}{4} - \frac{f}{2} \tag{12}$$

An alternative geometric proof of (12) may be of interest. The family of ellipses passing through A and B has smallest major axis, and hence minimum energy, when the vacant focus is at the midpoint of the joining chord. Thus the chord is the latus rectum and the tangent line at the extremity has slope $\tan\theta=e$. But it is easily seen that $e=\frac{\cos f}{1+\sin f}=\tan(\frac{\pi}{4} - \frac{f}{2})$.

W is symmetric about θ_{ME}. This can be seen by defining

$$\delta\theta \equiv \theta - \theta_{ME}$$

Equation (10) can then be written

$$W = -\tan(\theta_{ME}+\delta\theta)\ \tan(\theta_{ME}-\delta\theta)$$

Figure A1 plots V vs. θ for f=1.25°. In this figure, retrograde ellipses, which actually occur for $\pi-f/2 < \theta \leq \pi$, are indicated by negative θ.

A comparison with the flat moon solution (dashed curve in Figure A1) is of interest. Equation (3) of the main text can be written

$$V = V_{ME}\ \sqrt{\csc 2\theta}$$

where the minimum energy velocity for $\theta_{ME} = \frac{\pi}{4}$ is

$$V_{ME} = \sqrt{xg}$$

$V_{ME,flat}$ is only 12.4 fps less than $V_{ME,curved}$. More generally if equation (11) is expanded into a Taylor's series for small f, one can show that for $\theta >> \tan^{-1} f$

$$V_{curved} \simeq V_{flat} \sqrt{1-f\cot\theta}$$

Trajectory time of flight t can be obtained from Kepler's equation. Let E be the eccentric anomaly corresponding to f (i.e., π-E is the "true" eccentric anomaly for π-f, for the posigrade ellipses*). Then

$$t = 2\sqrt{\frac{a^3}{\mu}} \; (E+e\sin E) \tag{13}$$

Now

$$\cos E = \frac{\cos f - e}{1 - e \cos f} \tag{14}$$

so that from (9)

$$\cos E = \frac{\cos(\theta+f)}{\cos \theta} \tag{15}$$

Also from (6), (10), and (15)

---

*To obtain the long arc of retrograde ellipses, E should be replaced by π-E in (13); and similarly for (18).

$$e \sin E = \frac{\sin \theta}{\sin(\theta+f)} \sqrt{1 - \frac{\cos^2(\theta+f)}{\cos^2 \theta}} \tag{16}$$

$$= \sqrt{1 - W^2 \sin \theta} \tag{17}$$

Equation (13) can then be written

$$t = 2\sqrt{R_0^3/\mu}\ (1-W)^{-3/2}\left[\arccos \frac{\cos(\theta+f)}{\cos \theta} + \sqrt{1-W^2}\ \sin \theta\right] \tag{18}$$

Figure A2 plots t vs. θ. The minimum, which occurs when $\theta=0$, is $t_{min} = 2f\sqrt{R_0^3/\mu} = 45.2$ sec. The retrograde circular orbit is t_{min} less than the orbital period $P = 2\pi\sqrt{R_0^3/\mu} = 108.4$ min. For the minimum energy ellipse $t_{ME} = 5.17$ minutes. The dashed curve shows the flat moon solution, namely (cf. equation (4) of the main text)

$$t = t_{ME}\ \sqrt{\tan \theta}$$

where

$$t_{ME} = \sqrt{2x/g}$$

$t_{ME,flat}$ turns out to be only 4.4 seconds less than $t_{ME,curved}$.

2. Impact Densities

Suppose that the distributions of velocity, azimuth, and elevation of the ejected particles are given, say d(V), $q(\phi)$, and $p(\theta)$, respectively. For simplicity we assume that these distributions are mutually independent. If N_T is the total number of particles it is convenient to normalize the

velocity distribution so that

$$\int_{V_{min}}^{V_{max}} d(V)dV = N_T$$

Since the density of particles passing through a surface element $dS(=\cos\theta d\theta d\phi)$ of a unit hemisphere centered at the LM is $q(\phi)p(\theta)\cos\theta d\theta d\phi$, we also have

$$\int_{-\pi}^{\pi} q(\phi)d\phi = 1$$

$$\int_{0}^{\pi/2} p(\theta)\cos\theta d\theta = 1$$

If the distributions are isotropic in direction and uniform in velocity (denoted by the subscript 0), then

$$p_0(\theta) = 1$$

$$q_0(\phi) = \frac{1}{2\pi} \qquad (19)$$

$$d_0(V) = \frac{N_T}{V_{max}-V_{min}}$$

Assuming initially a flat moon, we wish to determine the number of particles impacting within a small square of

side Δ about the PSE (with coordinates (D,0)--see figure below)

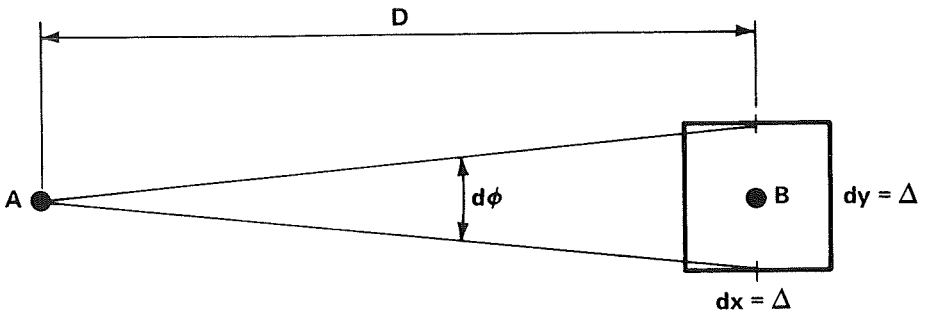

and within a small time interval about t, say $(t-\tau/2,\ t+\tau/2)$. Note that when making the transformation between ejection variables (V,θ,ϕ) and impact variables (x,y,t), the differential elements transform according to

$$d\phi \simeq \frac{1}{x}\, dy \qquad , \qquad \text{for } |y| \text{ small}$$

$$dV d\theta = J dt dx$$

where J is the Jacobian

$$J = \frac{\partial(V,\theta)}{\partial(t,x)}$$

When the transformation is in the form

$$V = V(\theta,x)$$

$$t = t(\theta,x)$$

then it is easy to verify* that

$$J = \frac{\partial V}{\partial x} \Big/ \frac{\partial t}{\partial \theta} \tag{20}$$

The number of impacting particles can now be written

$$\int_{t-\tau/2}^{t+\tau/2} \int_{D-\Delta/2}^{D+\Delta/2} \int_{-\Delta/2}^{\Delta/2} d(V)p(\theta)q(\phi)\,\frac{\cos\theta}{x}\,J(t,x)\,dt\,dx\,dy \simeq N(t)\cdot\tau\Delta^2$$

where the (weighted) particle impact density, N(t), is given by

$$N(t) = \frac{1}{D}\,d(V)p(\theta)q(0)\cos\theta\;J(t,D) \tag{21}$$

with V and θ expressed in terms of t and D.** If d(V), p(θ), and q(ϕ) are all uniform, (equations (19)), one gets the unweighted particle impact density

$$n(t) = \frac{N_T}{V_{max}-V_{min}} \cdot \frac{1}{2\pi D}\cos\theta \cdot J(t,D) \tag{22}$$

The weighted density can then be written as

$$N(t) = \frac{d(V)}{d_0(V)} \cdot \frac{q(0)}{q_0(0)} \cdot p(\theta) \cdot n(t) \tag{23}$$

since $p_0(\theta)=1$.

---

*A formalistic proof is as follows: $dV=V_\theta d\theta+V_x dx$, $dt=t_\theta d\theta+t_x dx$. Hence $(dV-V_\theta d\theta)t_\theta d\theta=V_x dx(dt-t_x dx)$. Dropping terms in $d\theta^2$ and dx^2 gives $dVd\theta=V_x/t_\theta dxdt$.

**If the azimuth of the PSE is ϕ_0, then in (21) q(0) is replaced by $q(\phi_0)$.

The preceding analysis is easily modified to treat the impacting energy rather than number of particles.* Assuming that all particles have the same mass m, then the energy density--unweighted and weighted--is simply

$$e(t) = \frac{m}{2} V^2 \cdot n(t)$$
$$E(t) = \frac{m}{2} V^2 \cdot N(t) \qquad (24)$$

where V is evaluated at t, D.

For a spherical moon the variable x is replaced by the central angle f, and the nominal distance D by F. In addition

$$\left.\frac{\partial V}{\partial x}\right|_{x=D} = \left(\frac{\partial V}{\partial f} \cdot \frac{\partial f}{\partial x}\right)\Bigg|_{f=F} = \frac{1}{2R_0} \cdot \left.\frac{\partial V}{\partial f}\right|_{f=F}$$

For a flat moon we find easily that $J=\cos\theta/t_{ME}^2$, whence

$$n(t) = n_{ME} \cdot 2\cos^2\theta$$
$$= n_{ME} \frac{2}{1+(t/t_{ME})^4} \qquad (25)$$

where n_{ME}, the particle density for the minimum energy trajectory is given by

$$n_{ME} = \frac{N_T}{V_{max}-V_{ME}} \cdot \frac{g}{8\pi D^2} \qquad (26)$$

---

*The extension to (energy)$^{\alpha}$ is trivial. One can also allow for variable distribution of mass, and even for seismic response that depends on the distance of the particle impact from the PSE.

The energy density is

$$e(t) = e_{ME} \cdot \cot\theta$$

$$= e_{ME}(t/t_{ME})^{-2} \tag{27}$$

where, from (24) and (26),

$$e_{ME} = \frac{m}{2} V_{ME}^{2} n_{ME}$$

$$= \frac{N_T}{V_{max}-V_{ME}} \cdot \frac{mg^2}{16\pi D} \tag{28}$$

For a curved moon we get, after algebraic simplification,

$$\left.\frac{\partial V}{\partial f}\right|_{f=F} = \frac{dV}{dW} \cdot \left.\frac{\partial W}{\partial f}\right|_{f=F}$$

$$= \frac{1}{2}\sqrt{\frac{\mu}{R_0}}\,\frac{1}{\sqrt{1+W}}\,\frac{\tan\theta}{\sin^2(\theta+F)} \tag{29}$$

$$\left.\frac{\partial t}{\partial \theta}\right|_{f=F} = \sqrt{\frac{R_0^{\,3}}{\mu}}\;\frac{\csc(\theta+F)}{(1-W)} \cdot \left\{\frac{3}{2}\sqrt{\frac{\mu}{R_0^{\,3}}}\; t \sec\theta\left(\frac{\sin}{\sin(\theta+F)} - \frac{\cos(\theta+F)}{\cos\theta}\right)\right.$$

$$\left. + 2\,\frac{\sin F}{\sqrt{1+W}}\,(\sec^2\theta + 1 + W)\right\} \tag{30}$$

whence

$$\frac{n(t)}{n_{ME}} = \frac{F(1-W)\ \sin\theta/\sin\ (\theta+F)}{\frac{3}{2}\cdot(t\sqrt{\mu/R_0^3})\ \sqrt{1+W}\ \sec\theta\left[\frac{\sin}{\sin(\theta+F)} - \frac{\cos(\theta+F)}{\cos\ \theta}\right] + 2\sin F(\sec^2\theta+1+W)} \tag{31}$$

where $n_{ME} = n_{ME,flat}$ is the flat moon density at minimum energy, given by (26). The actual density for the curved moon is

$$n_{ME,curved} = n_{ME,flat} \cdot \frac{F\ \cot\ F}{(1\ +\ \sin\ F)^2}$$

The energy density can be similarly derived. The left side of (31) replaces n by e, while the right side is multiplied by (1+W)/F. We also get

$$e_{ME,curved} = e_{ME,flat} \cdot \cos\ F/(1+\sin F)^3$$

Suppose now that the distribution of ejected particles is anisotropic, with $p(\theta)$ given by

$$p(\theta) = (k+1)\ \sin^k\theta \tag{32}$$

The effect of azimuth enters only in the constant factor $q(0)$,† and hence does not affect the analysis. Assuming $d(V)$ to be uniform, we get from (23)

$$N(t) = (k+1)\ \sin^k\theta \cdot n(t)$$

$$E(t) = (k+1)\ \sin^k\theta \cdot e(t) \tag{33}$$

---

†Or $q(\phi_0)$--compare footnote on page A 8.

Comparatively simple expressions are obtained in the case of a flat moon. From (25) and (27) we get

$$N(t) = C(k+1)\ \sin^{k}\theta\ \cos^{2}\theta$$

$$= C(k+1)\,(t/t_{ME})^{2k}\,[1+(t/t_{ME})^{4}]^{-(1+k/2)} \qquad (34)$$

$$E(t) = C(k+1)\sin^{k-1}\ \theta\ \cos\ \theta$$

$$= C(k+1)\,(t/t_{ME})^{2k-2}\ [1+(t/t_{ME})^{4}]^{-k/2} \qquad (35)$$

For $N(t)$, the maximum occurs at $t=t_{ME}(k/2)^{1/4}$; for $E(t)$, at $t=t_{ME}(k-1)^{1/4}$.

The above analysis can be inverted. Given the actual seismogram record, say $S(t)$, one can determine the angular distribution $p(\theta)$ required to produce $S(t)$, for t exceeding the minimum arrival time. Using a number density criterion, and assuming uniform distribution of velocities, one has

$$p(\theta) = \frac{S(t)}{n(t)} \qquad (36)$$

This equation provides merely the relative density--the proper magnitude is obtained by an appropriate choice of Δ, the distance about the PSE for which particle impacts are considered significant; τ, time unit for reckoning impact density; and N_T, total number of ejected particles. Similarly, using an energy density criterion,

$$p(\theta) = \frac{S(t)}{e(t)} \qquad (37)$$

The effect of non-uniform velocity distribution d(V) of ejected particles can be analyzed mathematically in a similar manner. However, because of the symmetric behavior of velocity about the minimum energy ellipse, the seismogram cannot be explained for both the early and the late portions solely through a velocity distribution. Given any d(V) one can clearly determine the corresponding angular distribution $p(\theta)$ required to fit the observed seismogram. Indeed, the two distributions need not be independent, since only those V-θ combinations which produce admissible trajectories affect the response at the PSE.

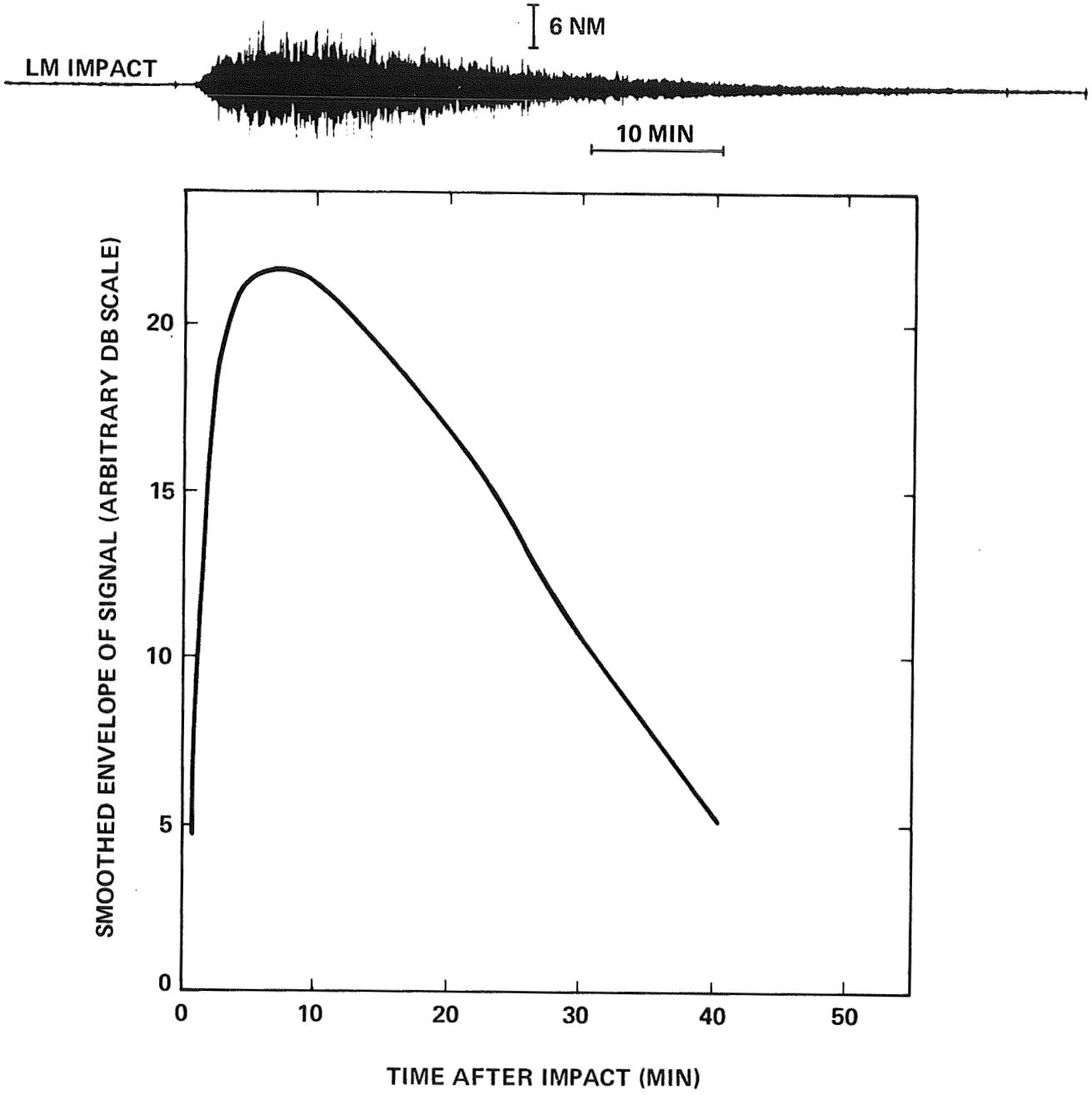

FIGURE 1 - SEISMIC SIGNAL RECEIVED ON THE LONG-PERIOD VERTICAL COMPONENT SEISMOMETER FROM THE LM IMPACT (FROM LATHAM, et al, REFERENCE 3)

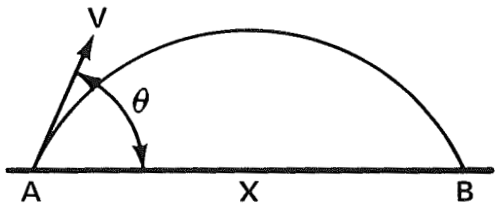

FLAT MOON CASE

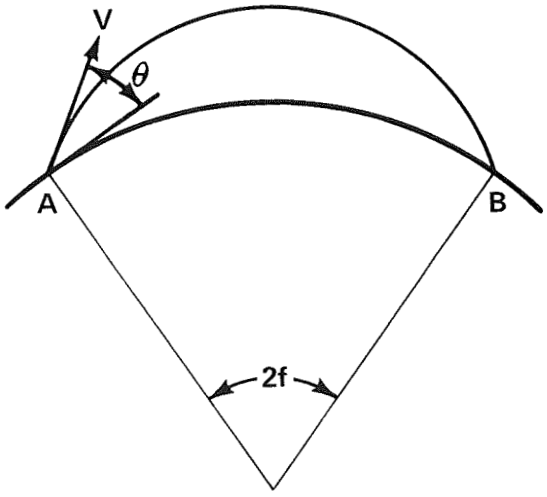

CURVED MOON CASE

FIGURE 2 - TRAJECTORY GEOMETRY

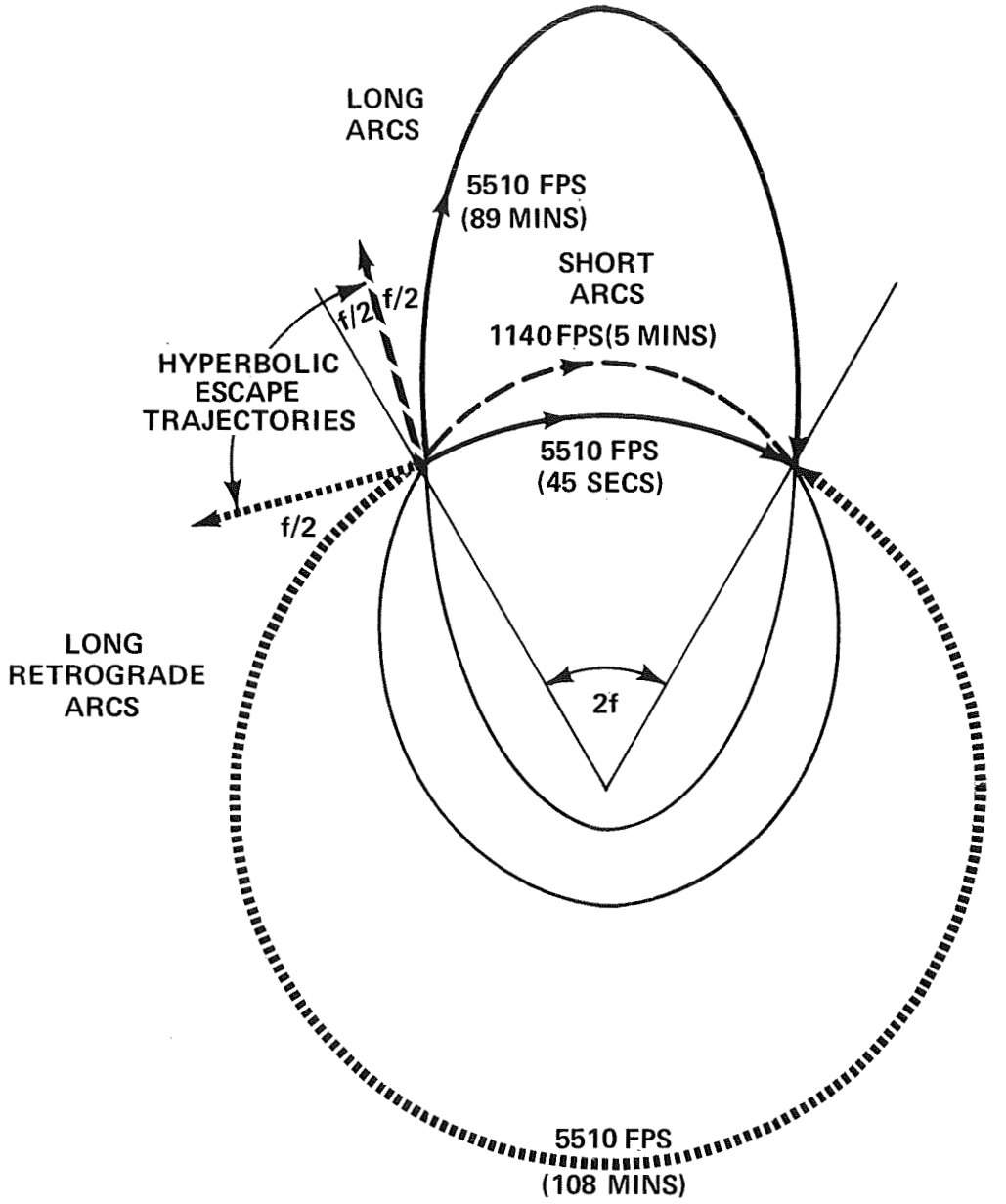

FIGURE 3 - POSSIBLE TRAJECTORIES CONNECTING THE LM AND THE SEISMOMETER

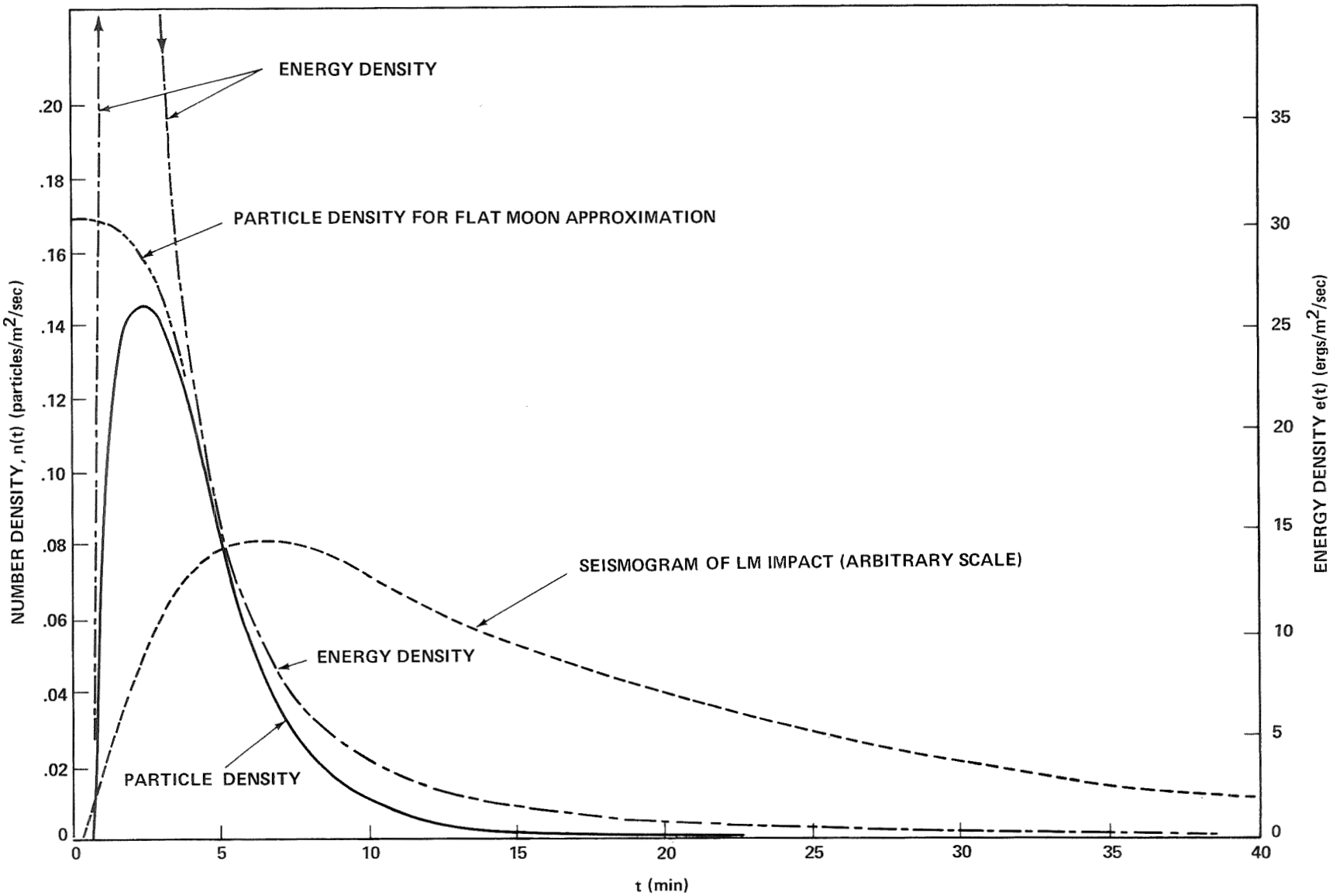

FIGURE 4 - PARTICLE AND ENERGY DENSITY FOR ISOTROPIC DISTRIBUTION

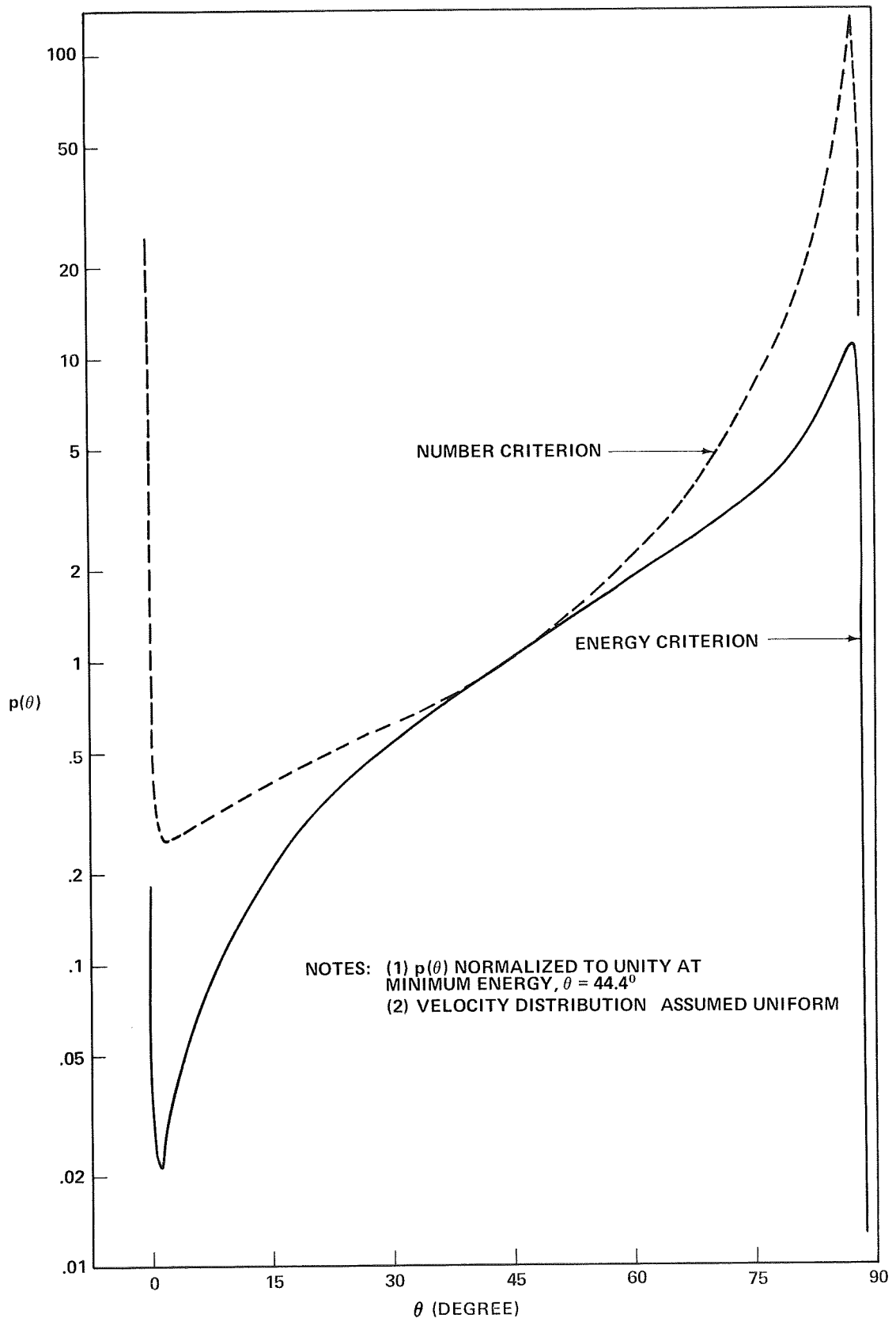

FIGURE 5 - ANGULAR DISTRIBUTION p(θ) REQUIRED TO FIT SEISMOGRAM

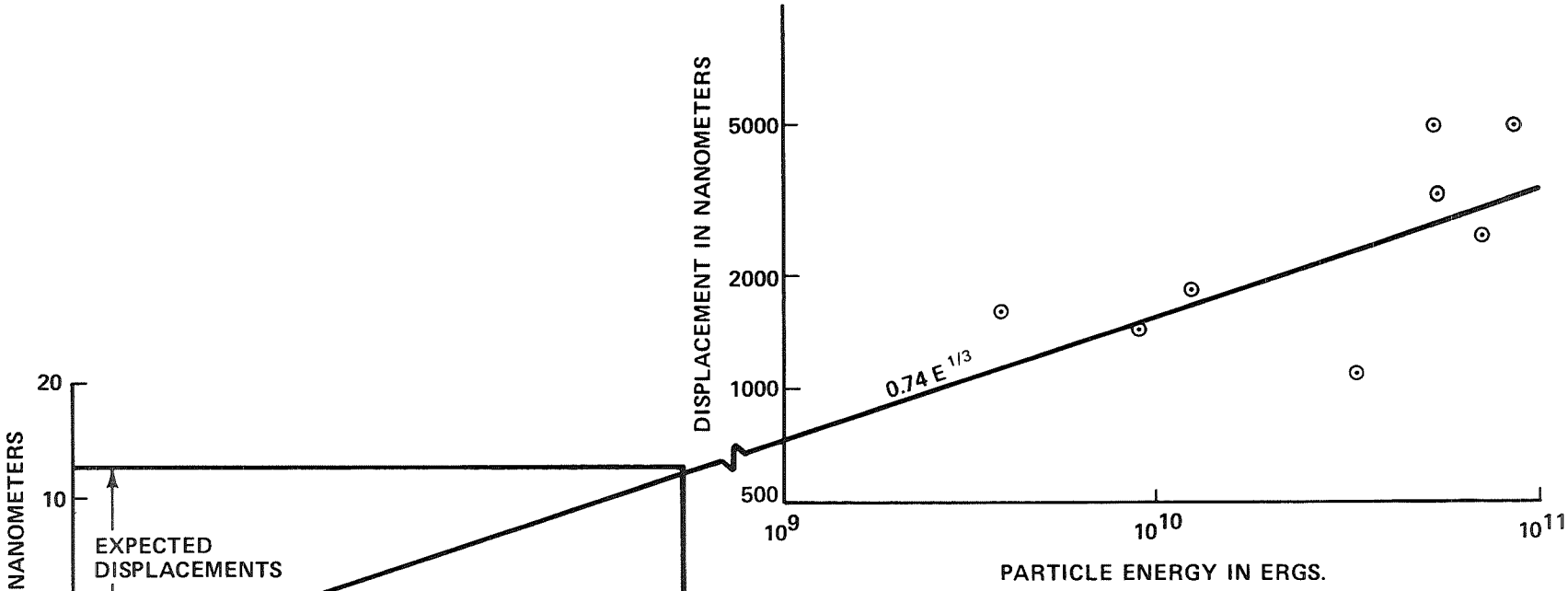

FIGURE 6A - DISPLACEMENT VS. PARTICLE ENERGY (EXPERIMENTAL)

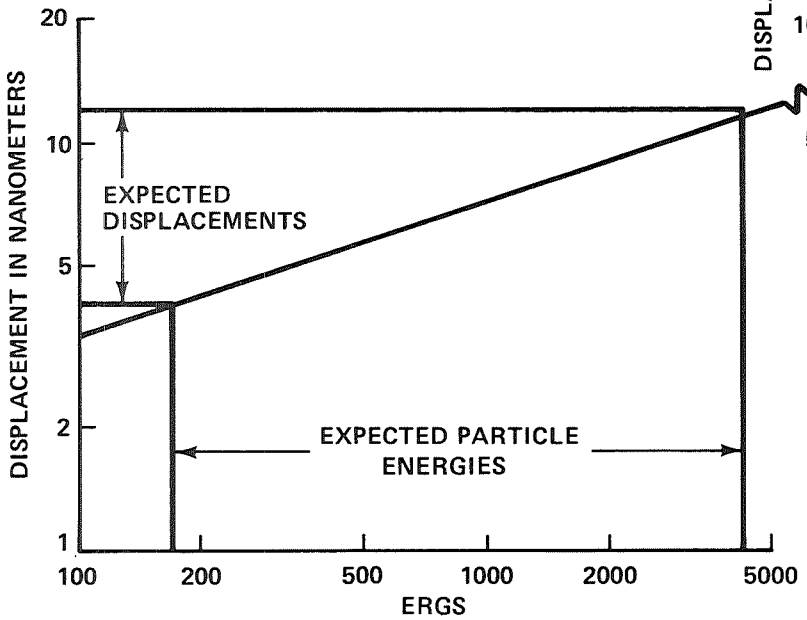

FIGURE 6B - DISPLACEMENT VS. PARTICLE ENERGY (EXTRAPOLATION)

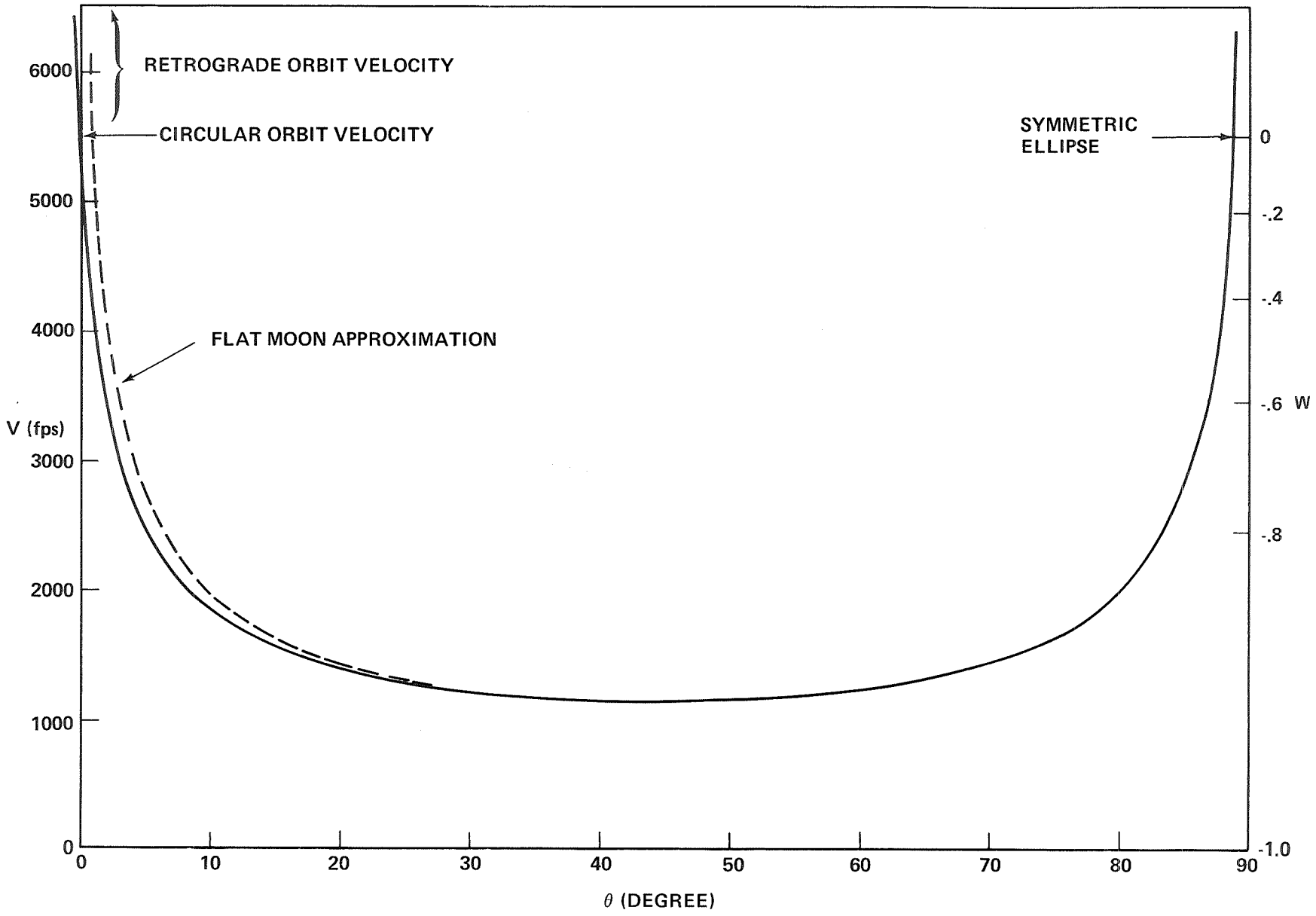

FIGURE A1 - REQUIRED VELOCITY TO IMPACT AT PSE VS. EJECTION ANGLES

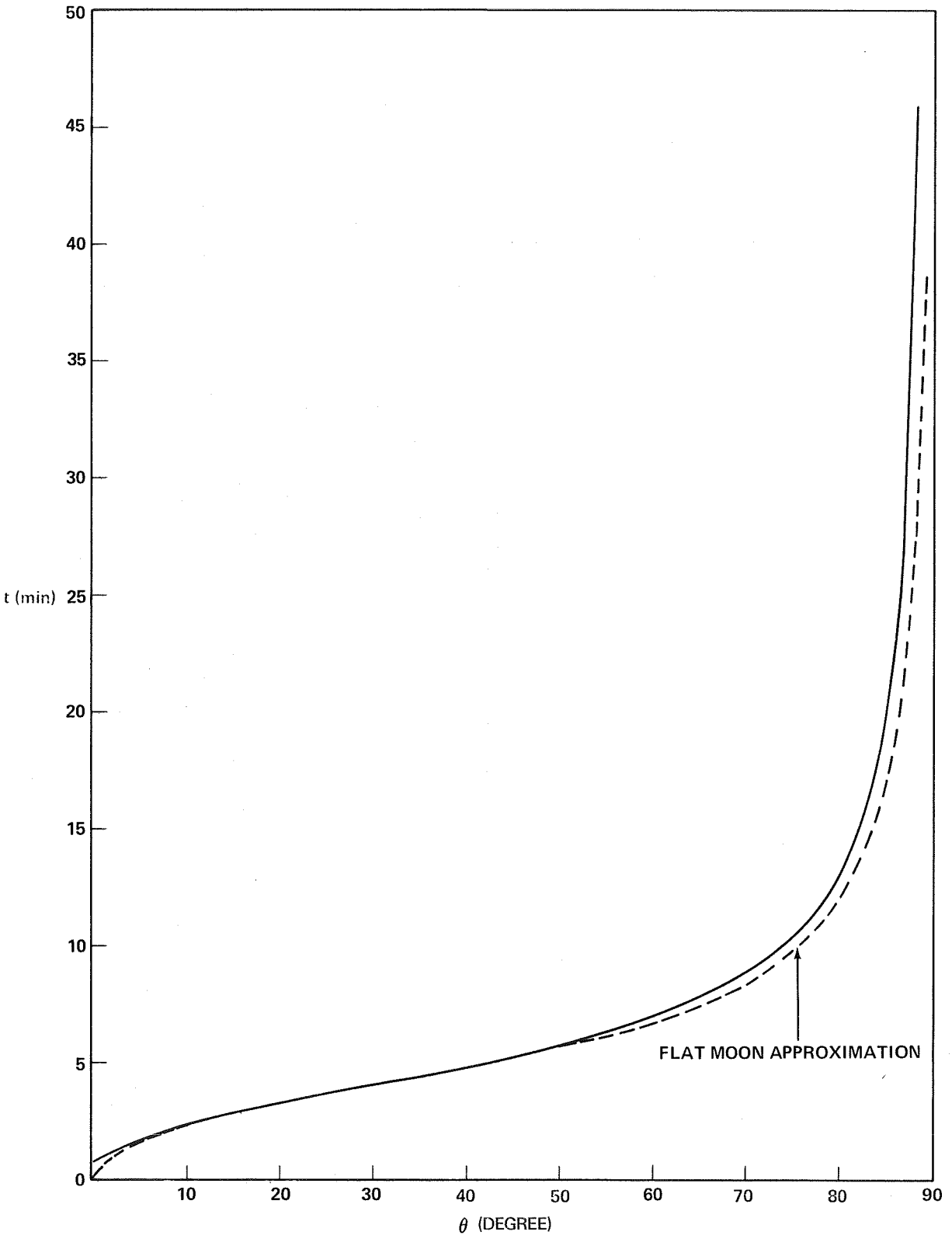

FIGURE A2 – FLIGHT TIME VS. EJECTION ANGLE